Tikrit Journal of Engineering Sciences (2025); 32(2): 1890
DOI: http://doi.org/10.25130/tjes.32.2.3

IRAQI Academic Scientific Journals

ISSN: 1813-162X (Print); 2312-7589 (Online)
Tikrit Journal of Engineering Sciences
available online at: http://www.tj-es.com

TJES Tikrit Journal of Engineering Sciences

Comparative Study of Activated Carbon and Silver Nanoparticle-Loaded Activated Carbon Derived from Tea Waste for Removal of Tetracycline from Aqueous Solution

Hala A. Faisal [a], Alaa Kareem Mohammed [*a], Nadya Hussin AL Sbani [b], Wan Nor Roslam Wan Isaha [c]

a University of Baghdad, AL Khwarizmi College of Engineering, Biochemical Engineering Department, Baghdad 47024, Iraq.
b Department of Chemical Engineering, Faculty of Oil and Gas Engineering, Al Zawia University, Libya.
c Department of Chemical and Process Engineering, Faculty of Engineering and Built Environment, Universiti Kebangsaan Malaysia, 43600 UKM Bangi, Selangor, MALAYSIA.

Keywords:
Adsorption; Adsorption kinetics; Central Composite Design; Isotherms model; Tea residue.

Highlights:

- *Producing activated carbon from tea residue.*
- *Applying silver nanoparticles onto the produced activated carbon.*
- *Utilizing the produced activated carbon and silver nanoparticle-loaded activated carbon to remove tetracycline (TC) contaminants from artificially polluted water.*
- *Comparing the effectiveness of activated carbon and activated carbon loaded with AgNps in removing total coliforms (TC) from water contaminated.*

ARTICLE INFO
Article history:

Received	25 Nov. 2023
Received in revised form	15 Jan. 2024
Accepted	07 Mar. 2024
Final Proofreading	05 Mar. 2025
Available online	16 May 2025

Citation: Faisal HA, Mohammed AK, AL Sbani NH, Isaha WNRW. **Comparative Study of Activated Carbon and Silver Nanoparticle-Loaded Activated Carbon Derived from Tea Waste for Removal of Tetracycline from Aqueous Solution**. *Tikrit Journal of Engineering Sciences* 2025; **32**(2): 1890.
http://doi.org/10.25130/tjes.32.2.3

*Corresponding author:

Alaa Kareem Mohammed
University of Baghdad, AL Khwarizmi College of Engineering, Biochemical Engineering Department, Baghdad 47024, Iraq.

Abstract: The present work elucidates the utilization of activated carbon (AC) and activated carbon loaded with silver nanoparticles (AgNPs-AC) to remove tetracycline (TC) from synthetically polluted water. The activated carbon was prepared from tea residue and loaded with silver nanoparticles. Scanning electron microscopy (SEM), X-ray diffraction (XRD), Fourier transform infrared spectroscopy (FTIR), and Brunauer-Emmett-Teller (BET) were used to characterize the activated carbon (AC) and silver nanoparticles-loaded activated carbon (AgNPs-AC). The impact of various parameters on the adsorption effectiveness of TC was examined. These variables were the initial adsorbate concentration (Co), solution acidity (pH), adsorption time (t), and dosage of the adsorbent. The maximum TC removal percentage was (88%) at pH = 9, time = 230 min, Co = 60 ppm, and dosage = 0.39 g/25 ml using AC as an adsorbent. Whereas the maximum TC removal percentage was (98%) at pH = 9, time = 46 min, Co = 60 ppm, and dosage = 0.0406 g/25 ml using AgNPs-AC. The isotherm models were also studied. It was found that the Langmuir isotherm model fitted well with the experimental data. The adsorption kinetics study showed that the pseudo-second-order accurately describes the experimental results. The analysis of the adsorption thermodynamics revealed that TC adsorption on TAC and AgNPs-AC was endothermic and spontaneous. The study aims to make activated carbon from tea waste and load silver nanoparticles on that activated carbon (AgNPs-AC). It also studies how two adsorbents (activated carbon and activated carbon loaded with silver nanoparticles) remove tetracycline from artificially polluted water. Then, the outcomes were compared.

دراسة مقارنة للكاربون المنشط والكاربون المنشط المحمل بجسيمات الفضة النانوية المشتق من بقايا الشاي لإزالة التتراسيكلين من المحلول المائي

هالة علي فيصل[1]، علاء كريم محمد[1]، ناديا حسين السباني[2]، وان نور رسلام وان عيسى[3]

[1] كلية الخوارزمي للهندسة/ قسم الهندسة الكيميائية الحيوية/ بغداد – العراق.

[2] قسم الهندسة الكيميائية/ كلية هندسة النفط والغاز/ جامعة الزاوية/ ليبيا.

[3] قسم الهندسة الكيميائية وهندسة العمليات/ كلية الهندسة والبيئة العمرانية/ جامعة كيبانغسان ماليزيا/ UKM ٤٣٦٠٠ بانجي/ سيلانغور- ماليزيا.

الخلاصة

يوضح العمل الحالي استخدام الكاربون المنشط والكاربون المنشط المحمل بجسيمات الفضة النانوية لإزالة التتراسيكلين(TC) من المياه الملوثة صناعيًا، تم تحضير الكربون المنشط من بقايا الشاي المستخدم وتحميله بجزيئات الفضة النانوية. تم استخدام الفحص المجهري الإلكتروني (SEM) ,حيود الأشعة السينية (XRD), التحليل الطيفي للأشعة تحت الحمراء لتحويل فوريير (FTIR) و Brunauer-Emmett-Teller (BET). لوصف كل من الكاربون المنشط والكاربون المنشط المحمل بجزيئات الفضة النانوية. تم فحص تأثير المعلمات المختلفة على فعالية الامتزاز لـ TC. هذه المتغيرات هي تركيز المادة الممتزة الأولي (Co)، الدالة الحامضية للمحلول (pH)، وزمن الامتزاز (t)، وجرعة المادة المازة. تم العثور على الحد الأقصى لنسبة إزالة TC (٨٨٪) عند الدالة الحامضية = ٩ والوقت = ٢٣٠ دقيقة وتركيز اولي = ٦٠ جزء في المليون والجرعة = ٠,٣٩ جم / ٢٥ مل عند استخدام الكاربون النشط كمادة ماصة، في حين تم العثور على الحد الأقصى لنسبة إزالة TC عند الرقم الهيدروجيني = ٩ الوقت = ٤٦ دقيقة وتركيزاولي= 60 جزء في المليون، والجرعة = ٠,٠٤٠٦ جم/٢٥ مل عند استخدام AgNPs-AC. تم دراسة isothermوتبين أن نموذج Langmuir.يتناسب بشكل جيد مع البيانات التجريبي. أظهرت دراسة حركية الامتزاز أن الدرجة الثانية الزائفة تصف بدقة النتائج التجريبية. يكشف تحليل الديناميكا الحرارية للامتزاز أن امتزاز TC على TAC وAgNPs-AC هو ماص للحرارة وتلقائي.

الكلمات الدالة: الامتزاز، حركية الامتزاز، تصميم المركب المركزي، نموذج خطوط تساوي الحرارة، بقايا الشاي.

1.INTRODUCTION

Various pollutants are currently continuously contaminating the Earth's ecosystem [1]. One of the biggest environmental problems facing the community is the harmful chemical contamination of water resources, especially when those resources are the sole reliable source of drinking water [2, 3]. Pharmaceutical products are among the most important environmental pollutants discharged into water systems in large quantities by various human activities, including direct discharge from companies and hospitals, home sewage, effluents from water treatment facilities, and sewage treatment facilities [4, 5]. Due to the rising use of antibiotics, pharmaceutical effluents containing antibiotics have recently attracted a lot of interest [6, 7]. Extended exposure to very small amounts of antibiotics can develop antibiotic-resistant genes. The usage of antibiotics has rapidly increased, raising worries about their environmental residues [8, 9]. Tetracycline antibiotics (TC) are the second most commonly used antibiotics in the world due to their low cost, broad-spectrum antibacterial activity, and significant therapeutic efficacy [10]. It is frequently used to treat animal illnesses and is added to animal diets to promote growth [11, 12]. Tetracycline is commonly found in wastewater due to its frequent use. Since TC is difficult to biodegrade, it poses a serious risk to people and the environment [13]. Therefore, removing TC residues from effluents before releasing them into the environment is required [14]. Tetracycline can be eliminated using various techniques, including electrochemical approaches, membrane filtration, reverse osmosis, advanced oxidation, ozonation, and biological therapies. Most of these techniques are more expensive, resulting in the development of by-products, or are less effective. It is necessary to search for a more suitable and practical strategy to remove antibiotics [15]. Among the above methods, adsorption technologies have been widely applied. remove pharmaceuticals from surface water; adsorption technology is a very effective, user-friendly, and globally advanced treatment approach. This technique of treatment uses synthetic or natural materials (known as sorbents, adsorbents, or biosorbents) to remove pollutant molecules (also known as adsorbates) from contaminated fluids [16]. Many porous materials have been investigated for the adsorption of tetracycline, including resin, silica, clay, multi-walled carbon nanotubes, zeolite, graphene oxide, chitosan, and activated carbon [17]. Activated carbon effectively and affordably adsorb various pharmaceutical contaminants from wastewater due to its high surface area, pore structure, and high capacity adsorption [18, 19]. It contains a non-graphitic and microcrystalline type of carbon. Non-graphitic means a substance with a high concentration of oxygen or a low concentration of hydrogen in its structure. The structure of activated carbon includes micropores, mesopores, and macropores. These structures greatly show how well-activated carbon works as an adsorbent [20]. Commercial activated carbon is one of the most frequently used industrial adsorbents; however, it is expensive. Therefore, to create inexpensive activated carbons, researchers are looking for suitable natural raw materials. These raw materials must also be affordable and easily accessible. Thus, by-products or residue from industry and agriculture are the primary raw materials that can be transformed into activated carbon [21] because they are readily available, inexpensive, and renewable, such as rice husk, sugarcane bagasse, maize husk, residual oil fly ash, olive

stones, banana stems, date stones, bamboo, waste newspapers, coconut shells, and tea dregs [22, 23]. Recently, using nanomaterials has also substantially increased scientific interest. Nanoparticles were employed as an effective adsorbent to remove contaminants from water and wastewater due to their very high surface area. However, nanomaterials are expensive, and their use in treating wastewater is fairly limited. Therefore, research should concentrate on combining nanomaterials with inexpensive adsorbents to lower treatment costs, expand using nanomaterials in removing contaminants [24], and create a novel modified material for removing pollutants from aqueous solutions to increase the adsorption capacity of adsorbents. Activated carbon doped with nanoparticles is a useful material with several uses, mostly for adsorption and antibacterial activity. For greater adsorption capacity, nanoparticles can improve the active sites of activated carbon (AC) [25, 26]. The present study aims to prepare activated carbon from tea residue and load silver nanoparticles onto activated carbon derived from tea residue (AgNPs-AC). Additionally, it examines the activity of two adsorbents (activated carbon and silver nanoparticles-loaded activated carbon) in removing tetracycline from synthetically polluted water and compares the results.

2.MATERIALS AND METHODS

2.1.Materials

The tea residue was collected locally from leftover tea used in homes. Tetracycline (TC) was selected as the target adsorbate, provided by the State Enterprise for Drug Industries and Medical Appliances, Samara, Iraq. Tetracycline was used directly without any further treatment. Silver nitrate ($AgNO_3$, purity > 99%), used as the precursor to create silver nanoparticles, and potassium hydroxide (KOH), employed as an activator, were purchased from Merk (Darmstadt, Germany). Borohydrate and starch were purchased from Sigma-Aldrich, USA.

2.2.Preparation of Activated Carbon

Waste tea was rinsed multiple times with hot distilled water until it was colorless, then dried at 110 °C in an air oven for 10 hours to eliminate any remaining water-soluble components. The raw material was then placed in a steel or ceramic crucible and heated in a furnace to 350 °C for 30 minutes while exposed to a flow of N_2 (150 cm^3/min) for carbonization. The product was then permitted to cool inside the furnace while nitrogen gas continued to flow until the temperature reached 100 °C before being removed. The carbonized material was then mixed with 30% KOH at a ratio of 2:3 w/w (KOH: carbonized material) and agitated at 140 rpm for 30 minutes. The sample was subsequently filtered to remove the base residue and deposited in a closed crucible in a muffle furnace at 900°C for one hour with a nitrogen flow (150 cm^3/min). The product was then allowed to cool to room temperature under the same nitrogen flow. The obtained activated carbon (AC) was thoroughly washed with distilled water until the solution became neutral (pH = 7). The AC samples were dried at 110 °C for 24 h, then crushed with a mortar and pestle, and sieved to a particle size of 350 µm or less. The last AC particle samples were maintained in a desiccator for the next batch of experiments.

2.3.Synthesis of Silver Nanoparticles

The synthesis of silver nanoparticles was conducted utilizing a hydrothermal technique using silver nitrate ($AgNO_3$) [27]. In the experimental setup, a quantity of 0.2 grams of starch was mixed with a volume of 100 mL of $AgNO_3$ solution with a concentration of 0.001 M. Consequently, the starch solutions, including Ag^+ ions' production, were observed. Following this, the mixture underwent extensive agitation (450 rpm) at a temperature of 70 °C using a magnetic stirrer for 3 hr to achieve a state of homogeneity. A 0.001 M solution of sodium borohydride was gradually added to a combination with a volume of 25 mL while maintaining the solution temperature at 70 °C. The ultimate solution was allowed to cool to ambient temperature to facilitate subsequent utilization. Figure 1 shows the UV-vis absorption spectra of the Ag nanoparticles at different time intervals (10, 20, 30, 60, and 90 min). Typical AgNPs have λ max values, which are in the visible range of 400-500 nm [28]. The absorption peak of obtained AgNPs is centered around 410-430 nm. This observation clearly indicates the successful reduction of Ag using soluble starch. The weight percent of the prepared Ag NPs in the solution was about 0.0136%. The Surface Plasmon peak observed confirmed the influence of starch in reducing Ag+ ions to Ag NPs from an aqueous $AgNO_3$ solution. Forming AgNPs increased with reaction time. A wide beak at a short reaction time (10 min) was observed due to the presence of a wide distribution particle size. A slight modification in the size and shape of nanoparticles gave a slight shift in the peak to a shorter wavelength with increasing time [29]. From the figure, it is observed that the absorption peak becomes sharp as the time increases from 10-90 min, indicating the formation of the poly-dispersed AgNPs initially that become mono-dispersed spherical nanoparticles with increasing reaction time. Therefore, the mixing time at room temperature is a key factor in determining the size distribution of AgNPs.

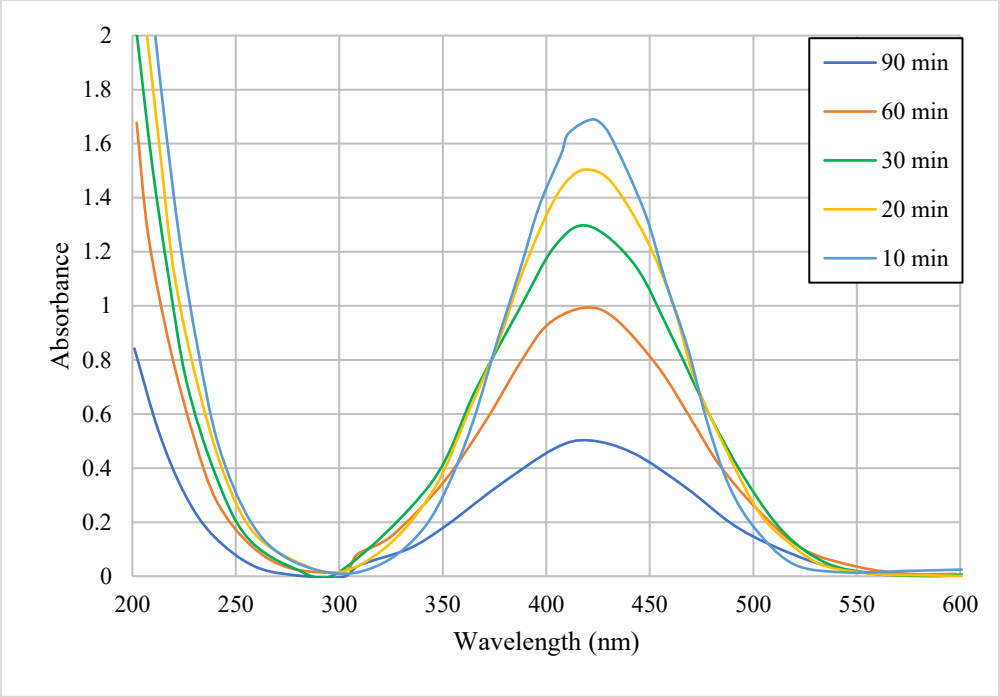

Fig. 1 UV-Vis Absorption Spectra of the Ag Nanoparticles.

2.4.Preparation of the AgNPs-Loaded Activated Carbon

The technique of wet impregnation was employed to load AgNPs onto tea-activated carbon (TAC) [27]. In 250-mL Erlenmeyer flasks, AgNPs and TAC were combined at a mass ratio of 35 w/w. The flasks were then shaken continuously for 24 hours at 120 rpm. After impregnation, the wet particles were filtered and dried for 2 h at 105 °C to produce modified TAC (AgNPs-TAC). The AgNPs-TAC was used in batch-mode adsorption experiments to remove tetracycline from aqueous solutions.

2.5.Characterization of Activated Carbon

Different characterizations were conducted to ascertain the properties of the activated carbon (AC) and silver nanoparticles-loaded activated carbon (AgNPs-AC). The scanning electron microscopy (SEM) technique was employed to examine the surface morphologies. (EDX) analysis was used to determine the component content of the absorbent. The specific surface area and pore volume of the prepared absorbent material were determined using a Brunauer-Emmett-Teller (BET) method. X-ray diffraction (XRD) was used to analyze the crystalline structure of the adsorbent. Fourier transform infrared spectroscopy (FTIR 8400s Shimadzu) was used to examine the surface functional groups of the adsorbent.

2.6.Adsorption Study

Adsorption studies were conducted with activated carbon and silver nanoparticles-loaded activated carbon to compare their efficiency in the adsorption of tetracycline. The batch experiments of tetracycline with activated carbon were implemented with different contact times (20-300 min), initial concentrations (30–150 mg/l), initial pH of the solution (2-11), and sorbent dosages (0.05-0.5 g/ 25 mL). While experiments of tetracycline with silver nanoparticles-loaded activated carbon were implemented with contact times (5-60 min), initial concentrations (30–150 mg/l), initial pH of the solution (2-11), and sorbent dosage (0.0125-0.05g/ 25 mL). To conduct these experiments, a specific amount of the adsorbent was added to 25 ml of the TC synthetic solution contained in a 100 ml Erlenmeyer flask. At 140 rpm, the mixture was agitated using an Edmund Buhler SM25 Orbital shaker (German). The concentration of tetracycline in each sample was evaluated using UV-visible absorption spectroscopy (PG Instruments, Model UV T80, England) following adsorption at various time intervals. The tetracycline samples were filtered using Whatman filter paper to separate them from the AC residue and get a solution devoid of carbon. The tetracycline removal efficiency and adsorption capacity were determined using Eqs. (1) and (2) [30].

$$R\,\% = \left[\frac{C_0 - C_e}{C_0}\right] * 100\% \quad (1)$$

$$q_e = \frac{(C_0 - C_e)V}{m} \quad (2)$$

where R% represents the removal percentage. C_o and C_e are initial and equilibrium concentrations of tetracycline (mg/ L), respectively. q_e is (TC) adsorbed amount (mg/g). V is the sample volume (ml), and m is the quantity of the adsorbent added (g).

Fig. 2 Setup of Experimental Work.

2.7.Experimental Design

For modeling and analyzing systems in which a variety of variables affect the response, Response Surface Methodology (RSM) is a widely used statistical and mathematical technique. It describes a set of statistical and experimental approaches that deal with one or more response variables. In this study, Central Composite Design (CCD) was used to plan the experiments, analyze, and study the effect of factors on tetracycline removal, as well as obtain an experimental model representing the removal process.

3.RESULTS AND DISCUSSION

3.1.Characterization of Adsorbent

3.1.1.Surface Morphology and Elemental Composition

Scanning electron microscopy (SEM) with energy dispersive X-ray spectroscopy (EDX) was used to characterize the surface morphological pictures and elemental composition of activated carbon and AgNPs-loaded activated carbon, as shown in Fig. 3 (a, b, c, and d).

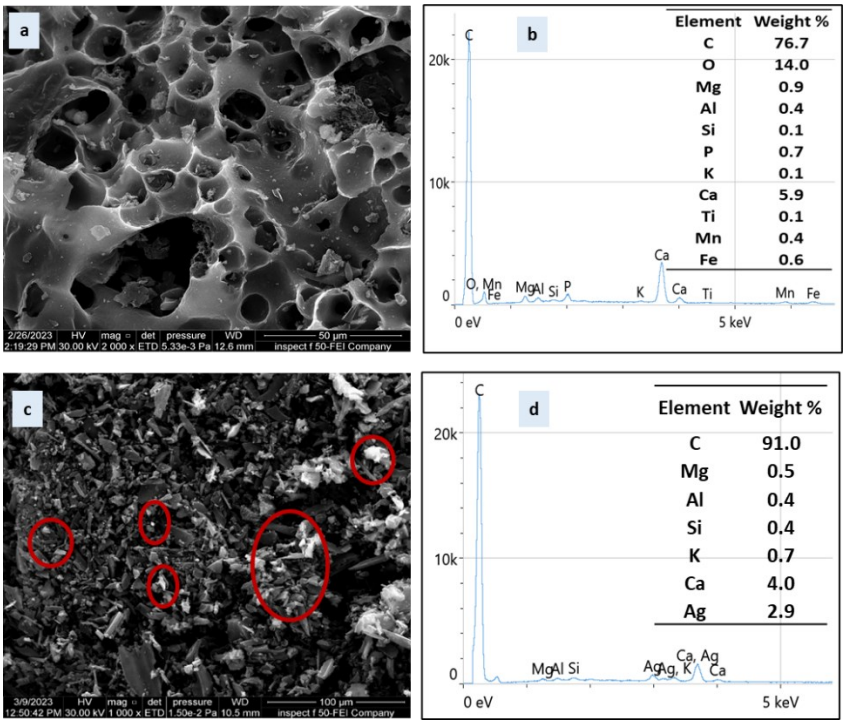

Fig. 3 SEM Micrographs and EDX Analysis of the Prepared Tea Residue Activated Carbon (a and b) and AgNPs-Loaded Activated Carbon (c and d).

Figure 3 (a) illustrates that the surface of the activated carbon exhibits a higher degree of roughness and is characterized by numerous holes, pores, cracks, and voids. These structural features of (AC) are likely related to the release of organic matter and utilization of carbon atoms during the chemical activation process. These results agree with Tao et al. [31], who prepared activated carbon from tea residue by NaOH activation. Figure 3 (c) displays the scanning electron microscope (SEM) picture of AgNPs-AC, revealing that the formation of AgNPs on the AC was caused by the presence of white beads on the surface of the AC, which is evidenced by the presence of white beads on the AC surface. The existence of these white beads significantly impacted the surface morphology of AgNPs-TAC. In scanning electron microscopy (SEM) images of tea-activated carbon (TAC), the white beads were not visible, which is evidence that the surface of AgNPs-TAC was coated with silver nanoparticles. The findings of the structural (SEM) analysis demonstrate agreement with the outcomes published by Trinh et al. [32] and Sikdar et al. [33]. EDX analysis was used to determine the elemental composition of types of adsorbents: activated carbon and activated carbon with AgNPs, as shown in Figs. 3 (b) and (d). The results showed that most of the total atomic composition (TAC) consisted of carbon (76.7%), oxygen (14%), calcium (5.9%), and magnesium (0.9%), as shown in Fig. 1 (b). The elemental composition of AgNPs-TAC, as depicted in Fig. 1 (d), consisted of the following proportions: carbon (91%), magnesium (0.5%), calcium (4%), silicon (0.4%), and silver (2.9%). These results show that the silver nanoparticles were successfully attached to the surface of the TAC material.

3.1.2.Brunaure, Emmett and Teller (BET)

Based on the Brunauer-Emmett-Teller (BET) analysis, the specific surface area of the activated carbon (AC) was 746.951 m^2/g, and the pore volume was 0.447 m^3/g. Upon loading the silver nanoparticles, the surface area and pore volume of the AgNPs-AC material increased to 820.512 m^2/g and 0.524 m^3/g, respectively. Devi et al. [34] also found similar results. They observed that the surface area of AC was 570.67 m^2/g and went up to 620 m^2/g when silver nanoparticles were added.

3.1.3.X-ray Diffraction (XRD)

The X-ray diffraction (XRD) investigation was conducted to confirm the crystalline structure of the particles present on the surface of the AC material. As seen in Fig. 4 (a), the presence of prominent X-ray diffraction (XRD) peaks at 32 and 44 degrees could potentially be ascribed to the diffraction phenomenon arising from the amorphous nature of AC. The diffraction peaks observed in Fig. 4 (b), occurring at 2θ angles of 38, 45, 65, and 78°, can be attributed to the diffraction phenomena exhibited by the face-centered-cubic silver planes denoted as (111), (200), (220), and (311), respectively. This observation provides evidence that the particles adhered to the activated carbon (AC) surface are composed of metallic silver (Ag^0) particles. In addition, it was observed that the peaks corresponding to amorphous carbon did not exhibit any shift, indicating that the loading procedure did not induce any modifications to the crystalline structure of the carbon material. Tang et al. also reported comparable findings [35].

3.1.4.Fourier Transform Infrared Spectroscopy (FTIR)

The FTIR spectra of tea, activated carbon (AC), and silver nanoparticles-loaded activated carbon (AgNPs-AC) are depicted in Fig. 5. In FTIR spectra of tea, the O-H stretching vibration of the hydroxyl group was responsible for the bandwidth at 3415.99 cm^{-1}. The peak at 2898.9 cm^{-1} resulted from the C-H stretching of the benzene ring. The presence of a methoxy group band in the precursor is responsible for the broadband at 2850.54 cm^{-1}. The bands at 1727.74 cm^{-1} and 1639.24 cm^{-1} were due to the chemical formula C = O for carboxymethyl cellulose [36]. The low absorption at 1524.37 cm^{-1} was due to the oscillation of the aromatic skeletal structure. The peak at 1458.07 cm^{-1} represented the carboxylic groups [37]. The bands between 1000 and 1300 cm^{-1} were produced by the C-C and C-O vibrations of alcohols, phenols, and ethers. The band at 588.86 cm^{-1} was caused by the Si-O-Si vibration [38]. FTIR spectra of AC and AgNPs-AC, the existence of the O-H stretch-bonded group is evident in Fig. 3, as indicated by the peaks observed at 3822, 3720, and 3406 cm^{-1}. The findings align with the observations made by Anisuzzaman et al. [39], wherein they noted that the O-H group exhibited peaks within the range of 3200–3800 cm^{-1}. The C=O stretching vibration in carbonyls, encompassing ketones, aldehydes, lactones, and carboxylic groups, was shown by a peak at 1669 cm^{-1}. Altintig et al. and Anisuzzaman et al. [39, 40] reported comparable findings. The peak corresponding to the C=C stretching vibration in aromatic rings was observed at a wavenumber of 1514 cm^{-1}, as reported by Foo and Hameed in their study conducted in 2009 [41]. The frequency at the prominent peak of 1050 cm^{-1} corresponds to the C-O stretching vibrations observed in carboxylic acids or lactone groups. Additionally, the presence of aromatic C-H bonds can be inferred from the peaks observed in the range of 581–841 cm^{-1}. The findings presented in this study exhibited a resemblance to the outcomes reported in the studies conducted by Anisuzzaman et al. [39], Altintig et al. [40], and Lazim et al. [42].

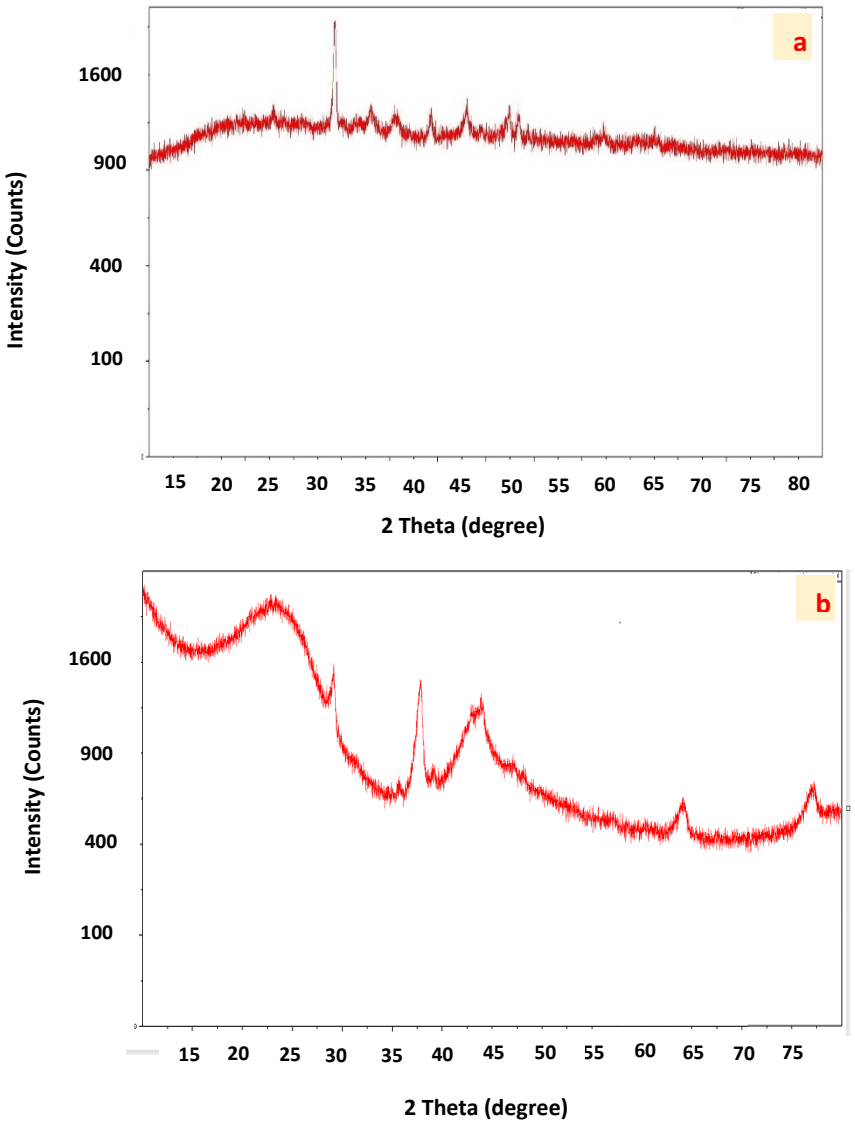

Fig. 4 XRD Analysis of (a) Activated Carbon and (b) AgNPs-Loaded Activated.

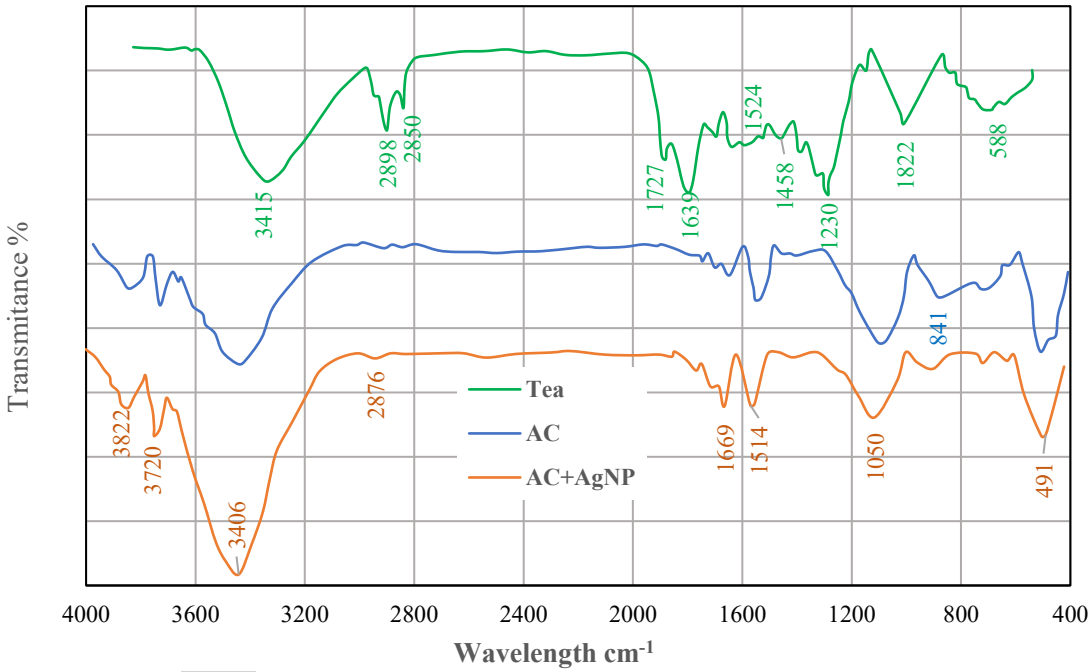

Fig. 5 FTIR Spectra of the Tea Residue, AC, and (AgNPs-AC).

3.2.Effects of Experimental Parameters on the Adsorption Process

3.2.1.Effect of Contact Time

The influence of time on removing the pollutant was examined using various time values, ranging from 20 to 300 min when using AC as an adsorbent and from 5 to 60 min when using AgNPs-AC. Tetracycline removal efficiency on AC, as shown in Fig. 6, increased with time until it achieved a constant value (88% removal) at 230 min. Removal of tetracycline on AgNPs-AC was comparable to that of TC on AC, and it was noted that removal of 98.8% was achieved after 46 min. The reason was that the surface of the adsorbent had many active sites available initially, which caused the fast adsorption. Adsorbate molecules filled more active sites as the process of adsorption advanced, which raised the resistance of tetracycline aggregation to diffuse deeper into the adsorbent and decreased the rate of adsorption until it reached equilibrium removal. In addition, the reason for the increase in removal rate when using AgNPs-AC as adsorbent at a time lower than the time when used AC as adsorbent was that the massive availability of active sites on the surface of AgNPs-AC than that found on the surface of AC and the higher tendency of AgNPs-AC toward binding TC through its functional group. This behavior agrees with Wong [43], who studied the removal of acetaminophen by adsorption on activated carbon synthesized from spent tea leaves. It was found that the amount of removal increased with time.

3.2.2.Effect of the Adsorbent Dosage

The effect of activated carbon and AgNPs-loaded activated carbon on the adsorption process was studied in the range of 0.05 – 0.5 and 0.0125-0.05 g per 25 ml of TC solution, respectively. Figure 7 shows the influence of adsorbent dose on TC removal percentage. As the adsorbent quantity increases, more active sites are exposed to TC molecules, and the removal percentage rises. However, the removal no longer increased after applying a certain amount of adsorbent. This amount can be considered the best adsorbent dosage, and it was 0.39 g / 25ml when used with AC and 0.0406 g/25ml when used with AgNPs-AC. These results conform with [41, 42].

3.2.3.Effect of pH

The effect of pH on the adsorption of tetracycline on activated carbon and AgNPs-loaded activated carbon was studied by varying the pH value from 2 to 11. It is clear from Fig. 8 that, with an increase in pH from 2 to 9, the removal efficacy significantly increased due to the competitive adsorption between relatively high concentrations of H+ ions and TC behaviors as cationic properties at lower pH values, which inhibits the adsorption of cationic TC on AC. In contrast, the increase in TC adsorption was attributed to the rise in the negatively charged AC surface with increasing OH concentration, enhancing the electrostatic attraction between negatively charged adsorbent and cationic TC molecules at higher pH values. These results conform with [46]. It was noticed that above pH 9, the efficiency of adsorption decreased due to higher solution pH, and the surface of the adsorbent was negatively charged; therefore, an electrostatic repulsion was formed between the surface of the adsorbent and TC, reducing the TC adsorption. This behavior is in agreement with [47].

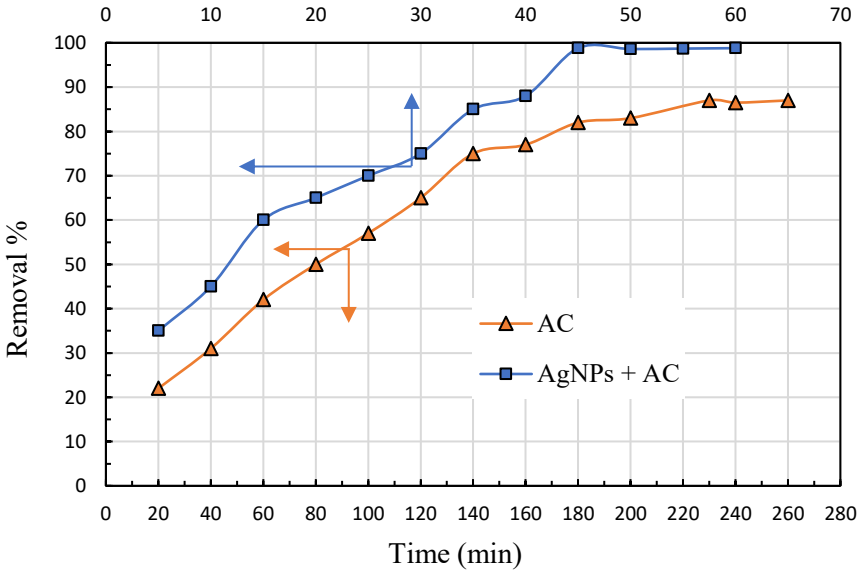

Fig. 6 Effect of Contact Time on Removal of Tetracycline.

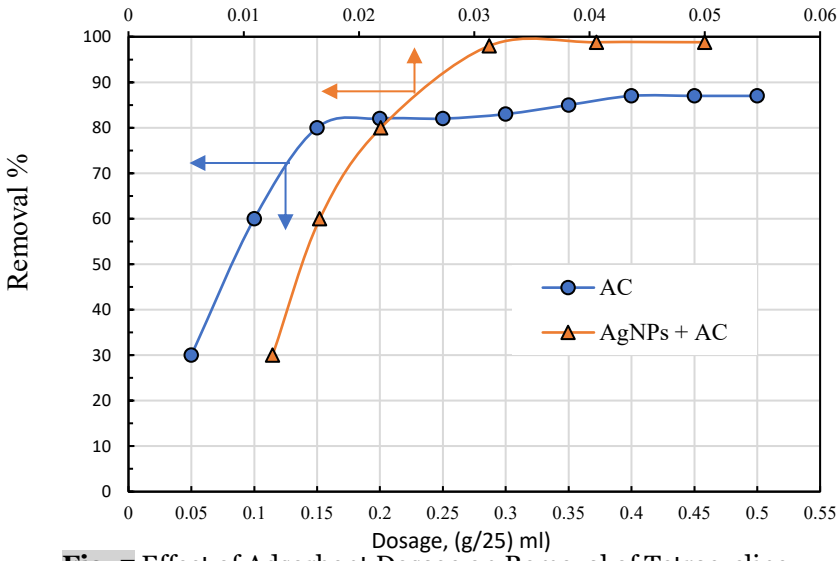

Fig. 7 Effect of Adsorbent Dosage on Removal of Tetracycline.

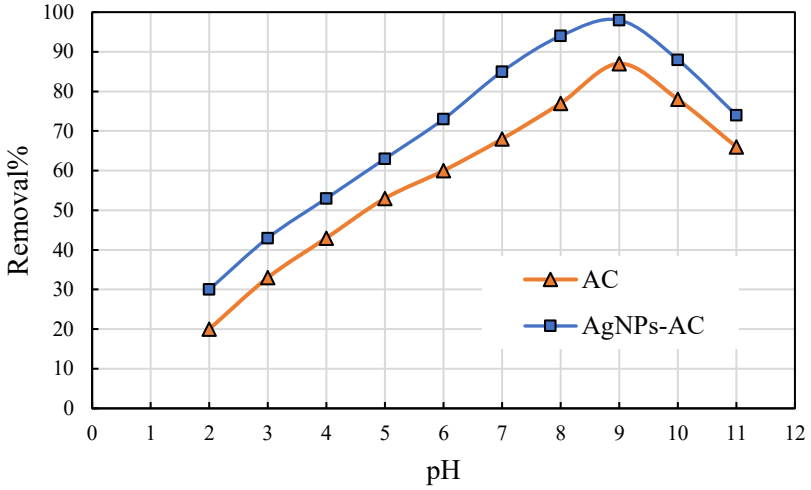

Fig. 8 Effect of pH on Removal of Tetracycline.

3.2.4.Effect of Initial Adsorbate Concentration

The initial TC concentration greatly affects the adsorption onto AC and AgNPs-AC. The range of initial adsorbate concentration values examined was 30-150 ppm. Figure 9 displays the impact of the initial concentration on TC removal. When the initial concentration increased from 30 to 60 ppm, the removal efficiency increased, but after that, the removal efficiency began to decrease. This phenomenon can be elucidated by the observation that, at lower concentrations of TC, the adsorption sites were not fully occupied. However, as TC increased, there was a greater chance that it would interact with active adsorbent sites. As a result, the higher TC content showed a larger percentage of removal. On the other hand, with a further increase in TC concentrations, the active sites of the same amount of adsorbent quickly got saturated, reducing the removal percentage. This behavior is similar to that observed by Adio [48], who investigated the removal of mercury from gas condensate using silver nanoparticle-loaded activated carbon as an adsorbent.

3.3.Central Composite Design Studies

In the present study, four important parameters, initial concentration, adsorbent dose, pH, and time, were chosen as the independent variables, while the removal of TC was selected as the response (dependent variable). Table 1 presents the independent factors with their actual levels selected for process optimization. The obtained experimental values were compared with the predicted values using CCD. The results found that the value of the adjusted coefficient R^2 was 0.9373, whereas the predicted value of R^2 was 0.8338. For the adsorption of TC on AgNPs-AC, the value of the adjusted coefficient R^2 was 0.9948, whereas the value that was predicted was 0.9869, suggesting the quadratic polynomial model is better than other models that have been tested. The polynomial model in quadratic form for the removal of TC on AC and AgNPs-AC is represented by Eqs. (3) and (4).

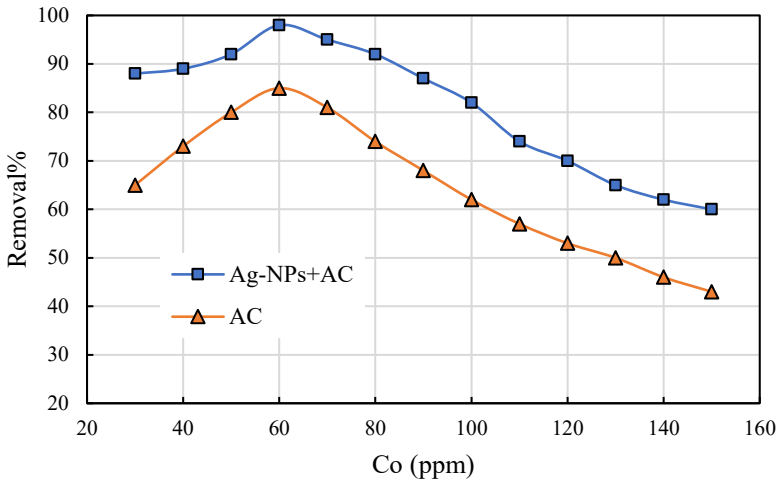

Fig. 9 Effect of Initial Concentration on Removal of Tetracycline.

Table 1 Variables and Levels Considered for the Percentage of Removal of TC on AC and AgNPs-AC.

	Independent factors			
	Contact time (A) (min)	**pH(B)**	**Adsorbent dosage(C) (g/25 ml)**	**Initial concentration(D) (ppm)**
Removal of TC on AC	20-300	2-12	0.05-0.5	30-150
Removal of TC on AgNPs-AC	5-60	2-12	0.0125-0.05	30-150

$$R\% = -125.73328 + 0.339777\,A + 21.73328\,B + 183.92869\,C + 1.20996D + 0.014021\,A\,B - 0.002659\,A\,D - 8.23037\,BC - 0.604944CD - 0.000541\,A^2 - 1.19067\,B^2 - 150.34321\,C^2 - 0.003503D^2 \quad (3)$$

$$R\% = 25.19019 + 0.573107\,A + 1.80789\,B + 1755.81145\,C + 0.223061D + 0.107879\,A\,B + 6.49697\,A\,C + 138.07407BC - 0.042778\,B\,D + 12.84444CD - 0.016383\,A^2 - 0.384691\,B^2 - 57002.66667\,C^2 - 0.002442D^2 \quad (4)$$

3.3.1.Interaction Between Adsorption Time and Initial Concentration of TC

Figure 10 shows the contour response surface of how adsorption time and initial TC concentration interact. Figure 10 (a) shows the interaction using AC as an adsorbent. From the contour plot (see red dots in the figure), the interaction area is enclosed in the rectangle (60–120 ppm and 90–230 min). Increasing contact time enhanced the removal percentage of TC, while increasing the initial concentration decreased the percent removal. The best values of percent removal (88%) occurred at Co = 60 ppm and Time = 230 min. Using AgNPs-AC as an adsorbent, the best value of percent removal (98.8%) occurred at Co = 60 ppm and Time = 46 min, as shown in Fig. 10 (b). These results show that adding silver nanoparticles to the activated carbon significantly increased the removal percentage of TC and cut down the time it took to reach this removal value. This observation can be attributed to the relationship between concentration and absorption time, where a higher concentration necessitates a longer absorption duration [49, 50].

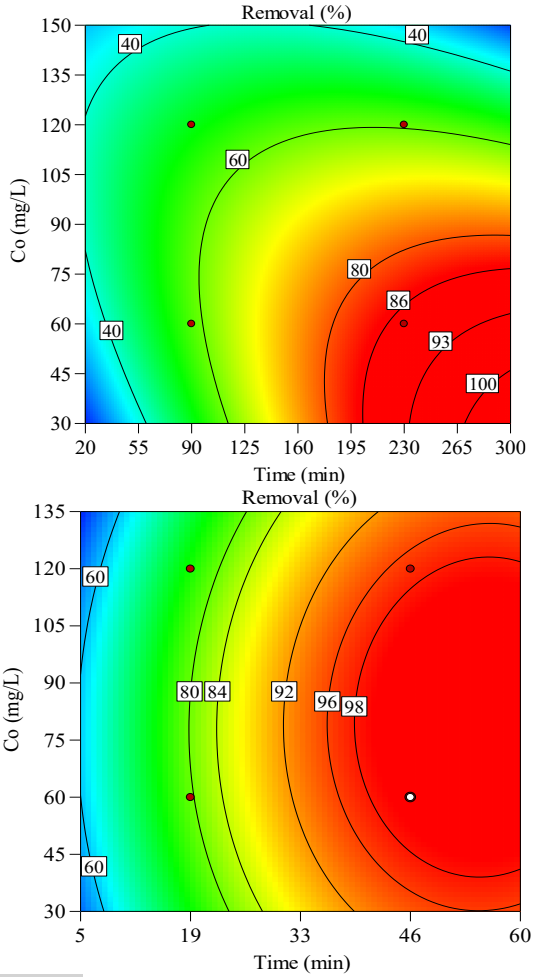

Fig. 10 Contour Plots of Removal Percent (%) of TC as a Function of Time (min) and Initial Concentration of TC (ppm) of (a) AC and (b) AgNPs-AC.

3.3.2.Interaction between pH and Adsorbent Dosage

Figure 11 displays the contour plot of the interaction between pH and adsorbent dosage. Figure 11 (a) shows the interaction using AC as an adsorbent. From the contour plot (red dots in Fig. 11 (a)), the interaction area is enclosed in the rectangle (4 -9 pH and 0.16-0.39 gm / 25 ml). Increasing the pH and adsorbent dosage increased the removal of TC until it reached a maximum removal of 88% at pH = 9 and 0.39 g/25 ml. Using AgNPs-AC as an adsorbent, the ranges of interacting variables were 4 -9 pH and 0.0219 - 0.0406 g/ 25 ml, as shown in Fig. 11 (b). The percent removal reached a maximum of 98.8% at a pH of 9 and an adsorbent dosage of 0.0406 g/25 ml. Loading Ag nanoparticles on the activated carbon enhances the removal of TC and decreases the amount of adsorbent used. This behavior is in agreement with [51].

3.4.Adsorption Isotherms

The experimental data are investigated using Freundlich and Langmuir isotherms to characterize the equilibrium relationship between adsorbent dosage and adsorbate uptake with time. Langmuir's hypothesis posits that adsorption occurs in a single layer on the surface of an adsorbent material, where there is no interaction between the adsorbate molecules. Furthermore, this adsorption occurs on a limited number of sites on the adsorbent, which possess uniform energies. Equation (5) represents the Langmuir isotherm model [52]:

$$\frac{1}{q_e} = \frac{1}{q_m} + \frac{1}{q_m K_a}\frac{1}{C_e} \qquad (5)$$

where q_e is the amount of sorbent adsorbed per unit mass at equilibrium(mg/g), q_m is the maximum adsorption capacity(mg/g), C_e is the equilibrium adsorbate concentration (mg/l), and K_a is the equilibrium constant of adsorption (l/mg). The Langmuir constants, q_m, and K_a, can be calculated from the slope and intercept of the 1/qe against 1/Ce plot. Freundlich isotherm adsorption assumes heterogeneous surfaces and multi-layer adsorption. Equation 6 presents the Freundlich isotherm [53].

$$\ln q_e = \ln K_F + (1/n)\ln C_e \qquad (6)$$

The Freundlich adsorption constant, denoted as K_F, represents the adsorption capacity in units of mg/g. The constant n is the Freundlich adsorption constant, measured in l/mg. The values of K_F and n, which represent the intercept and slope of the plot, respectively, can be determined by graphing the natural logarithm of q_e versus the natural logarithm of C_e. The graphical representation of the adsorption behavior of tetracycline on activated carbon (AC) and activated carbon loaded with silver nanoparticles (AgNPs-AC) can be observed in Figs. 12 (a, b) and 13 (a, b), respectively. The isotherm constants obtained from these plots are presented in Table 2.

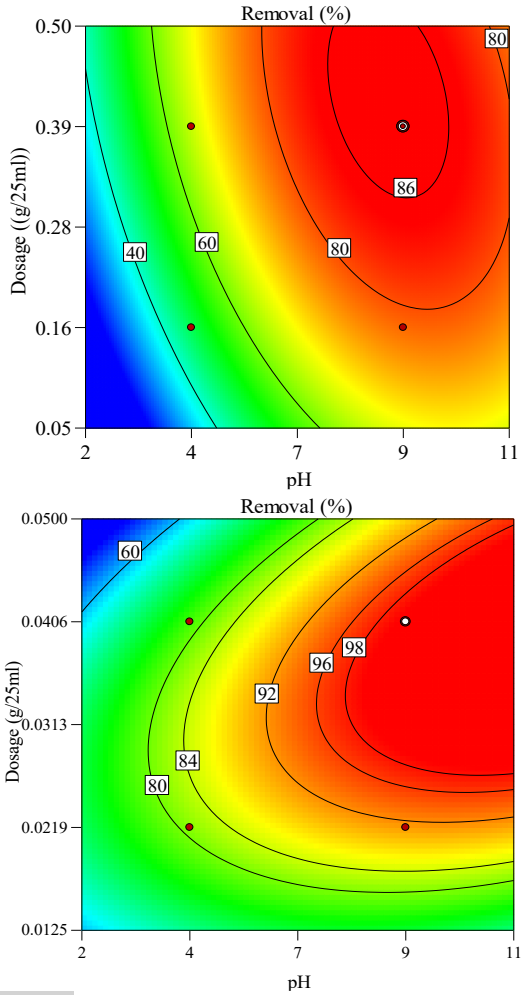

Fig. 11 Contour Plots of Removal Percent (%) of TC as a Function of pH and Adsorbent Dosage of (a) AC and (b) AgNPs-AC.

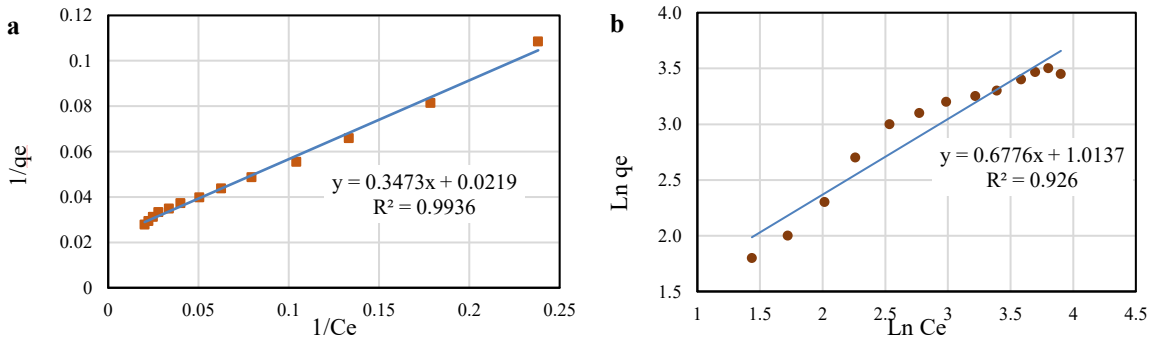

Fig. 12 A Linear form of the Isotherm Models for the Sorption of TC onto AC (a) Langmuir and (b) Freundlich.

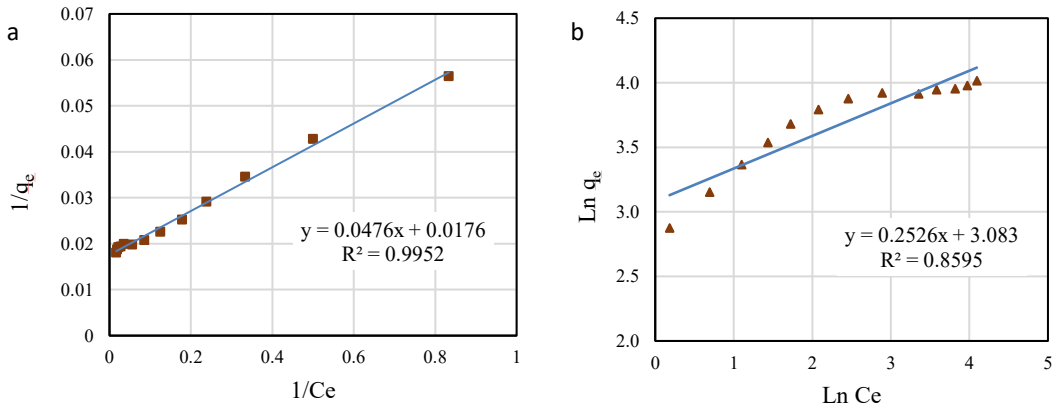

Fig. 13 A Linear form of the Isotherm Models for the Sorption of TC Onto AgNPs-AC (a) LANGMUIR and (b) Freundlich.

Table 2 Parameters of Langmuir and Freundlich Equations for Sorption of TC on AC and AgNPs-AC.

Model	Parameters	Adsorbent	
		AC	AgNPs-AC
Langmuir	q_m (mg/g)	45.662	5.682
	K_a (L/mg)	0.063	3.7
	R^2	0.9936	0.9952
Freundlich	K_f (mg/g)	1.644	1.29
	n	0.597	0.324
	R^2	0.9692	0.8595

It is observed from the data presented in Table 2 that the R^2 values of the Langmuir model were greater than those of the Freundlich model, indicating that the adsorption of TC on AC and AgNPs-AC was better described by the Langmuir model than by the Freundlich model, indicating monolayer adsorption in a suitable, homogeneous system.

3.5.Adsorption Kinetics

Several kinetic models are employed to describe the adsorbents' characteristics and evaluate the control mechanism. Two kinetic models, pseudo-first-order and pseudo-second-order, were used to examine the adsorption kinetics of tetracycline onto AC and AgNPs-AC. Eqs. (7) and (8) express the pseudo-first-order and pseudo-second-order models, respectively [54, 55].

$$\ln(q_e - q_t) = \ln(q_e) + k_1 \quad (7)$$

$$\frac{t}{q_t} = \frac{1}{k_2 q_e} + \frac{t}{q_e} \quad (8)$$

where q_e is the amount of pollution adsorbed at equilibrium(mg/g), $k_1(min^{-1})$ is the rate constant of the pseudo-first-order adsorption, $k_2(g/mg.min)$ is the rate constant of the pseudo-second-order adsorption, and q_t the amount of pollution adsorbed at time t (mg/g). Figures 14 and 15 show the kinetic model for the adsorption of TC on AC and AgNPs-AC. Table 3 shows all the factors and correlation coefficients (R^2) from the slope and intercept. Based on the correlation coefficients (R^2) shown in Table 4, the pseudo-second-order kinetic model best fits the experimental data for the adsorption of TC onto AC and AgNPs-AC.

3.6.Thermodynamic Study

Understanding thermodynamic characteristics is necessary to forecast whether the adsorption process will be feasible at a particular temperature. Three thermodynamic parameters, including enthalpy change (ΔH°), Gibbs free energy change (ΔG°), and entropy change (ΔS°), were used to examine how TC binds to AC and AgNPs-AC from a thermodynamic point of view. The thermodynamic parameters can be determined using Eqs. (9) and (10) [56, 57].

$$\Delta G^\circ = -RT \ln K_d \quad (9)$$

$$\ln K_d = \frac{\Delta S^\circ}{R} - \frac{\Delta H^\circ}{RT} \quad (10)$$

In this context, the symbol T represents the temperature in Kelvin, R (8.314 J /mol. K) denotes the gas constant, and K_d represents the thermodynamic equilibrium constant. The value of K_d can be determined using Eq. (11):

$$K_d = \frac{q_e}{c_e} \quad (11)$$

The variable qe is the amount of tetracycline adsorbed per unit weight of activated carbon (AC) and silver nanoparticles-loaded activated carbon (AgNPs-AC) at the equilibrium concentration, measured in milligrams per gram (mg/g). Meanwhile, Ce denotes the equilibrium concentration of tetracycline, expressed in milligrams per liter (mg/L). The Gibbs free energy change (ΔG°) was determined by calculations conducted at different temperatures. The values of standard entropy change (ΔS°) and standard enthalpy change (ΔH°) were obtained by utilizing the slope and intercept of the natural logarithm of the equilibrium constant $\ln K_d$ plotted against the

reciprocal of temperature (1/T), as depicted in Fig. 16. Table 4 summarizes the thermodynamic parameters ΔG°, ΔH°, and ΔS° at various temperatures for the adsorption of tetracycline onto AC and AgNPs-AC.

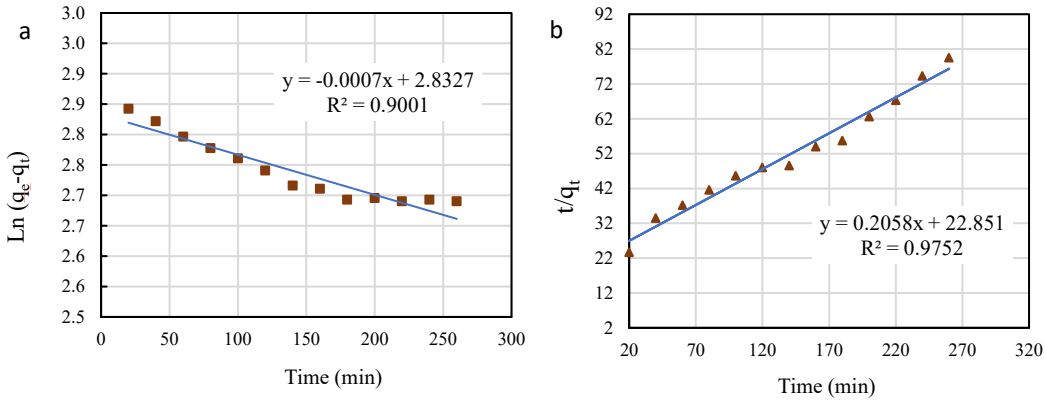

Fig. 14 Kkinetics Models for the Adsorption for Sorption of TC Onto AC, (a) Pseudo-First-Order and (b) Pseudo-Second-Order.

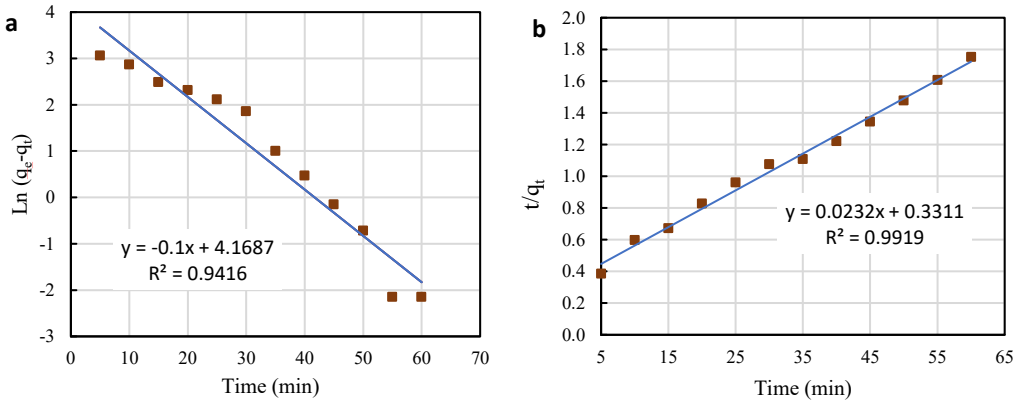

Fig. 15 Kinetics Models for Adsorption for Sorption of TC Onto AgNPs-AC, (a) Pseudo-First-Order and (b) Pseudo-Second-Order.

Table 3 Parameters of Adsorption Kinetics for Sorption of TC on AC and AgNPs-AC.

Model	Parameters	Adsorbent	
		AC	AgNPs-AC
Pseudo-first order	K_1 (min^{-1})	0.0007	0.1
	q_e (mg/g)	16.99	64.63
	R^2	0.9	0.9416
Pseudo-second order	K_2 (mg/g min)	0.0018	0.0016
	q_e (mg/g)	4.86	43.103
	R^2	0.9752	0.9919

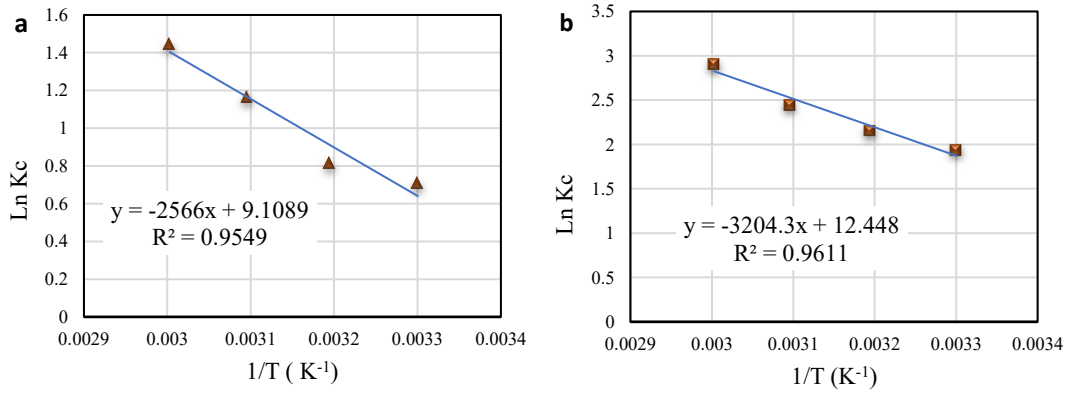

Fig. 16 ln K_d Versus $^1/_T$ for the Adsorption of TC Onto (a) AC and (b) AgNPs-AC.

Table 4 Thermodynamic Parameters for Sorption of TC on AC and AgNPs-AC.

Parameters		$\Delta G°$ (kJ/mol)				$\Delta S°$ kJ/mol K	$\Delta H°$ kJ/mol
Temperature		30 ^oC	40 ^oC	50 ^oC	60 ^oC		
Adsorbent	AC	-22.92	-23.68	-24.43	-25.19	75.73	21.333
	AgNPs-AC	-31.33	-23.68	-25.19	-8.038	103.49	26.64

The positive values of ΔH^o indicate an endothermic process, while the negative values of ΔG^o show a spontaneous and favorable process. The entropy change ΔS^o has a positive sign, revealing that the randomness at the interface of solid/liquid will increase during the adsorption of tetracycline.

4.CONCLUSION

The main objective of this study is to examine the sorption of TC from an aqueous solution utilizing AC and AgNPs-AC as two new environmentally friendly and nontoxic adsorbents. Tea residue was successfully transformed into activated carbon. Then, the activated carbon was successfully loaded with silver nanoparticles, which were used to effectively adsorb tetracycline from an aqueous solution. The adsorption of TC on the adsorbents was investigated using a batch method. The impact of several variables, including pH, number of adsorbents employed, contact time, and initial concentration, on the removal percentage of TC on both adsorbents was examined. It was found that the removal percentage of AgNPs-AC was high and quick. Compared to AC, the Ag-NP-AC had a high surface area, requiring less time and a smaller amount of adsorbent to remove. According to the isotherm analysis, the sorption data correlated well with Langmuir compared to the Freundlich isotherm model with (R^2= 0.9936) and (R^2 = 0.9952) for AC and AgNPs-AC, respectively. The pseudo-second-order model described the adsorption kinetics. Tetracycline adsorption on AC and AgNPs-AC was endothermic and spontaneous, according to a thermodynamics study.

ACKNOWLEDGMENTS

The authors would like to acknowledge and express their gratitude to the head and personnel of the biochemical engineering department at the Al-Khwarizmi College of Engineering, University of Baghdad, for their significant assistance in conducting the necessary laboratory measurements for this study. The authors would like to acknowledge the Petroleum Research and Development Centre (PRDC) for their assistance in characterizing and analyzing the samples. We would also like to express our gratitude to The State Enterprise for Drug Industries and Medical Appliances, Samara, Iraq, for providing us with tetracycline and other chemicals.

CONFLICT OF INTEREST STATEMENT

All authors declare that they have no conflicts of interest in disclosure.

REFERENCES

[1] Mohammed AA, Kareem SL. **Adsorption of Tetracycline from Wastewater by Using Pistachio Shell Coated with ZnO Nanoparticles: Equilibrium, Kinetic and Isotherm Studies.** *Alexandria Engineering Journal* 2019; **58**(3):917-928.

[2] Kareem SL, Mohammed AA. **Removal of Tetracycline from Wastewater Using Circulating Fluidized Bed.** *Iraqi Journal of Chemical and Petroleum Engineering* 2020; **21**(3):29-37.

[3] Abd Ali T. **Using Activated Carbon Developed from Iraqi Date Palm Seeds as Permeable Reactive Barrier for Remediation of Groundwater Contaminated with Copper.** *Al-Khwarizmi Engineering Journal* 2016; **12**(2):34-44.

[4] Debnath B, Majumdar M, Bhowmik M, Bhowmik KL, Debnath A, Roy DN. **The Effective Adsorption of Tetracycline onto Zirconia Nanoparticles Synthesized by Novel Microbial Green Technology.** *Journal of Environmental Management* 2020; **261** :110235, (1-13).

[5] Faisal AAH, Abdul MB, Alaa K, Mohammed K, Ghfar AA, Kareem MBA. **Novel Sorbent of Sand Coated with Humic Acid-Iron Oxide Nanoparticles for Elimination of Copper and Cadmium Ions from Contaminated Water.** *Journal of Polymers and the Environment* 2021; **29**(11):3618-3635.

[6] Yu F, Sun S, Han S, Zheng J, Ma J. **Adsorption Removal of Ciprofloxacin by Multi-Walled Carbon Nanotubes with Different Oxygen Contents from Aqueous Solutions.** *Chemical Engineering Journal* 2016; **285**:588-595.

[7] Kareem A, Israa M, Nadya MR, Al H. **Modification, Characterization of Tea Residue-Derived Activated Carbon, and Ciprofloxacin Adsorption.** *Al-Khwarizmi Engineering Journal* 2024; **20**(1):1-16.

[8] Barbooti MM, Zahraw SH. **Removal of Amoxicillin from Water by Adsorption on Water Treatment**

Residues. *Baghdad Science Journal* 2020; **17**(3):1071-1079.

[9] Rashid IM, Salman SD, Mohammed AK. **Removal of Pathogenic Bacteria from Synthetic Contaminated Water Using Packed Bed Silver Nanoparticle-Coated Substrates.** *Energy, Ecology and Environment* 2021; **6**(5):462-468.

[10] Liu S, et al. **Ultra-High Adsorption of Tetracycline Antibiotics on Garlic Skin-Derived Porous Biomass Carbon with High Surface Area.** *New Journal of Chemistry* 2020; **44**(3):1097-1106.

[11] Ahmed MJ. **Adsorption of Quinolone, Tetracycline, and Penicillin Antibiotics from Aqueous Solution Using Activated Carbons: Review.** *Environmental Toxicology and Pharmacology* 2017; **50**:1-10.

[12] Dai Y, Li J, Shan D. **Adsorption of Tetracycline in Aqueous Solution by Biochar Derived from Waste Auricularia Auricula Dregs.** *Chemosphere* 2020; **238**:124432.

[13] Rashid IM, Alwared AI, Abdelkareem HN. **Biosorption of Cd(II) Ions by Chlorella Microalgae: Isotherm, Kinetics Processes and Biodiesel Production.** *Desalination and Water Treatment* 2023; **311**:67-75.

[14] Premarathna KSD, et al. **Clay-Biochar Composites for Sorptive Removal of Tetracycline Antibiotic in Aqueous Media.** *Journal of Environmental Management* 2019; **238**:315-322.

[15] Dutta J, Mala AA. **Removal of Antibiotic from the Water Environment by the Adsorption Technologies: A Review.** *Water Science and Technology* 2020; **82**(3):401-426.

[16] Jabbar NM, Salman SD, Rashid IM, Mahdi YS. **Removal of an Anionic Eosin Dye from Aqueous Solution Using Modified Activated Carbon Prepared from Date Palm Fronds.** *Chemical Data Collections* 2022; **42**:100965.

[17] Hameed HF, Mohammed AK, Zageer DS. **Comparative Study between Activated Carbon and Charcoal for the Development of Latent Fingerprints on Nonporous Surfaces.** *Al-Khwarizmi Engineering Journal* 2022; **18**(4):1-13.

[18] Salman SD, Rasheed IM, Ismaeel MM. **Removal of Diclofenac from Aqueous Solution on Apricot Seeds Activated Carbon Synthesized by Pyro Carbonic Acid Microwave.** *Chemical Data Collections* 2022; **43**: 100982.

[19] Mohammed AK, Hameed HF, Rashid IM. **Wastewater Remediation Using Activated Carbon Derived from Alhagi Plant.** *Desalination and Water Treatment* 2023; **300**:36-43.

[20] Yahya MA, et al. **A Brief Review on Activated Carbon Derived from Agriculture By-Product.** *AIP Conference Proceedings* 2018; 1972(1): 1-8.

[21] Talib KE, Salman SD. **Removal of Malachite Green from Aqueous Solution Using Ficus Benjamina Activated Carbon-Nonmetal Oxide Synthesized by Pyro Carbonic Acid Microwave.** *Al-Khwarizmi Engineering Journal* 2023; **19**(2):26-38.

[22] Waleed Khalid M, Salman SD. **Adsorption of Chromium Ions on Activated Carbon Produced from Cow Bones.** *Iraqi Journal of Chemical and Petroleum Engineering* 2019; **20**(2): 23-32.

[23] Faisal AAH, Nassir ZS. **Modeling the Removal of Cadmium Ions from Aqueous Solutions onto Olive Pips Using Neural Network Technique.** *Al-Khwarizmi Engineering Journal* 2016; **12**(3):1-9.

[24] Nguyen LH, et al. **Treatment of Hexavalent Chromium Contaminated Wastewater Using Activated Carbon Derived from Coconut Shell Loaded by Silver Nanoparticles: Batch Experiment.** *Water, Air, and Soil Pollution* 2019; **230**(3): 68.

[25] Mohd Mokhtar MA, et al. **Green Synthesis of Silver Nanoparticles Doped Activated Carbon for Rhodamine B Dye Adsorption.** *9th Conference on Emerging Energy & Process Technology 2021 (CONCEPT 2021);* Venue: Virtual: p. 1-8.

[26] Chowdhury A, Kumari S, Khan AA, Chandra MR, Hussain S. **Activated Carbon Loaded with Ni-Co-S Nanoparticle for Superior Adsorption Capacity of Antibiotics and Dye from Wastewater: Kinetics and Isotherms.** *Colloids and Surfaces A: Physicochemical and Engineering Aspects* 2021; **611**:125868.

[27] Van HT, Nguyen TMP, Thao VT, Vu XH, Nguyen TV, Nguyen LH. **Applying Activated Carbon Derived from Coconut Shell Loaded by Silver Nanoparticles to Remove Methylene Blue in Aqueous Solution.** *Water, Air, and Soil Pollution* 2018; **229**(12): 393, (1-14).

[28] Yakout SM, Mostafa AA. **A Novel Green Synthesis of Silver Nanoparticles Using Soluble Starch and Its Antibacterial Activity.** *International Journal of Clinical and Experimental Medicine* 2015; **8**(3):3538-3544.

[29] Bedre MD, Basavaraja S, Deshpande R, Balaji DS, Venkataraman A. **Preparation and Characterization of Polypyrrole Silver Nanocomposites via Interfacial Polymerization**. *International Journal of Polymeric Materials* 2010; **59**(8): 531-543.

[30] Salman SD, Rasheed IM, Mohammed AK. **Adsorption of Heavy Metal Ions Using Activated Carbon Derived from Eichhornia (Water Hyacinth).** *5th International Scientific Conference on Environment and Sustainable Development* 2021; Baghdad, Iraq/ Istanbul, Turkey: p. 1-14.

[31] Tao J, Huo P, Fu Z, Zhang J, Yang Z, Zhang D. **Characterization and Phenol Adsorption Performance of Activated Carbon Prepared from Tea Residue by NaOH Activation.** *Environmental Technology* 2019; **40**(2):171-181.

[32] Trinh VT, et al. **Phosphate Adsorption by Silver Nanoparticles-Loaded Activated Carbon Derived from Tea Residue.** *Scientific Reports* 2020; **10**(1): 1-13.

[33] Sikdar D, Goswami S, Das P. **Activated Carbonaceous Materials from Tea Waste and Its Removal Capacity of Indigo Carmine Present in Solution: Synthesis, Batch and Optimization Study.** *Sustainable Environment Research* 2020; **30**(1): 1-16.

[34] Devi TB, Mohanta D, Ahmaruzzaman M. **Biomass Derived Activated Carbon Loaded Silver Nanoparticles: An Effective Nanocomposite for Enhanced Solar Photocatalysis and Antimicrobial Activities.** *Journal of Industrial and Engineering Chemistry* 2019; **76**:160-172.

[35] Tang C, Hu D, Cao Q, Yan W, Xing B. **Silver Nanoparticles-Loaded Activated Carbon Fibers Using Chitosan as Binding Agent: Preparation, Mechanism, and Their Antibacterial Activity.** *Applied Surface Science* 2016; **394**:457-465.

[36] Jagtoyen M, Derbyshire F. **Activated Carbons from Yellow Poplar and White Oak by H3PO4 Activation.** *Carbon* 1998; **36**(7-8):1085-1097.

[37] Stankovich S, Piner RD, Nguyen SBT, Ruoff RS. **Synthesis and Exfoliation of Isocyanate-Treated Graphene Oxide Nanoplatelets.** *Carbon* 2006; **44**(15):3342-3347.

[38] Boehm HP. **Surface Oxides on Carbon and Their Analysis: A Critical Assessment.** *Carbon* 2002; **40**(2):145-149.

[39] Anisuzzaman SM, Joseph CG, Taufiq-Yap YH, Krishnaiah D, Tay VV. **Modification of Commercial Activated Carbon for the Removal of 2,4-Dichlorophenol from Simulated Wastewater.** *Journal of King Saud University – Science* 2015; **27**(4):318-330.

[40] Altintig E, Kirkil S. **Preparation and Properties of Ag-Coated Activated Carbon Nanocomposites Produced from Wild Chestnut Shell by ZnCl2 Activation.** *Journal of the Taiwan Institute of Chemical Engineers* 2016; **63**:180-188.

[41] Foo KY, Hameed BH. **Utilization of Biodiesel Waste as a Renewable Resource for Activated Carbon: Application to Environmental Problems.** *Renewable and Sustainable Energy Reviews* 2009; **13**(9):2495-2504.

[42] Lazim ZM, Hadibarata T, Puteh MH, Yusop Z. **Adsorption Characteristics of Bisphenol A onto Low-Cost Modified Phyto-Waste Material in Aqueous Solution.** *Water, Air, and Soil Pollution* 2015; **226**(3): 1-11.

[43] Wong S, et al. **Removal of Acetaminophen by Activated Carbon Synthesized from Spent Tea Leaves: Equilibrium, Kinetics and Thermodynamics Studies.** *Powder Technology* 2018; **338**:878-886.

[44] Marzbali MH, Esmaieli M, Abolghasemi H, Marzbali MH. **Tetracycline Adsorption by H3PO4-Activated Carbon Produced from Apricot Nut Shells: A Batch Study.** *Process Safety and Environmental Protection* 2016; **102**: 700-709.

[45] Ghaedi M, Karimi H, Yousefi F. **Silver and Zinc Oxide Nanostructures Loaded on Activated Carbon as New Adsorbents for Removal of Methylene Green: A Comparative Study.** *Human and Experimental Toxicology* 2014; **33**(9):956-967.

[46] Mu Y, Ma H. **NaOH-Modified Mesoporous Biochar Derived from Tea Residue for Methylene Blue and Orange II Removal.** *Chemical Engineering Research and Design* 2021; **167**:129-140.

[47] Takdastan A, et al. **Preparation, Characterization, and Application of Activated Carbon from Low-Cost Material for the Adsorption of Tetracycline Antibiotic from**

Aqueous Solutions. *Water Science and Technology* 2016; **74**(10):2349-2363.

[48] Adio SO, Rana A, Chanabsha B, BoAli AAK, Essa M, Alsaadi A. **Silver Nanoparticle-Loaded Activated Carbon as an Adsorbent for the Removal of Mercury from Arabian Gas-Condensate.** *Arabian Journal for Science and Engineering* 2019; **44**(7): 6285-6293.

[49] Zhu H, Chen T, Liu J, Li D. **Adsorption of Tetracycline Antibiotics from an Aqueous Solution onto Graphene Oxide/Calcium Alginate Composite Fibers.** *RSC Advances* 2018; **8**(5):2616-2621.

[50] Al-Alawy AF, Al-Abod EE, Kadhim RM. **Synthesis and Characterization of Magnetic Iron Oxide Nanoparticles by Co-Precipitation Method at Different Conditions.** *The Journal of Engineering* 2018; **16**:2597-2603.

[51] Ghaedi M, et al. **Removal of Methylene Blue by Silver Nanoparticles Loaded on Activated Carbon by an Ultrasound-Assisted Device: Optimization by Experimental Design Methodology.** *Research on Chemical Intermediates* 2018; **44**(5): 2929-2950.

[52] Fadhil OH, Eisa MY. **Removal of Methyl Orange from Aqueous Solutions by Adsorption Using Corn Leaves as Adsorbent Material.** *Journal of Engineering* 2018; **25**(16): 2597-2603.

[53] Fadhel OH, Eisa MY, Zair ZR. **Decolorizing of Malachite Green Dye by Adsorption Using Corn Leaves as Adsorbent Material.** *Journal of Engineering* 2021; **27**(2):1-12.

[54] Rashid IM, Salman SD, Mohammed AK, Mahdi YS. **Green Synthesis of Nickel Oxide Nanoparticles for Adsorption of Dyes.** *Sains Malaysiana* 2022; **51**(2): 533-546.

[55] Ahmed Jasim M, Mohammed Abbas A. **Adsorption of Malachite Green Dye by Bio-Micro-Adsorbent from Aqueous Solution at Different Temperatures.** *2nd International Science Conference* 2019; University of Kerbala, Iraq: p. 1-9.

[56] Salman SD, Rashid IM. **Production and Characterization of Composite Activated Carbon from Potato Peel Waste for Cyanide Removal from Aqueous Solution.** *Environmental Progress & Sustainable Energy* 2024; 43(1): e14260.

[57] Mohammed AK, Saadoon SM, Abd Ali ZT, Rashid IM, Al Sbani NH. **Removal of Amoxicillin from Contaminated Water Using Modified Bentonite as a Reactive Material.** *Heliyon* 2024; **10**(3): e24916, (1-15).